POLITECNICO DI TORINO
Repository ISTITUZIONALE

Comparison of Analytical and Numerical Methods for the Evaluation of the Flow Forces in Conical Poppet Valves with Direct and Reverse Flow

Original
Comparison of Analytical and Numerical Methods for the Evaluation of the Flow Forces in Conical Poppet Valves with Direct and Reverse Flow / Rundo, Massimo; Altare, Giorgio. - In: ENERGY PROCEDIA. - ISSN 1876-6102. - ELETTRONICO. - 126:(2017), pp. 1107-1114. (Intervento presentato al convegno ATI 2017 - 72nd Conference of the Italian Thermal Machines Engineering Association tenutosi a Lecce nel 6-8 settembre) [10.1016/j.egypro.2017.08.261].

Availability:
This version is available at: 11583/2686277 since: 2017-10-16T09:15:56Z

Publisher:
Elsevier

Published
DOI:10.1016/j.egypro.2017.08.261

Terms of use:

This article is made available under terms and conditions as specified in the corresponding bibliographic description in the repository

Publisher copyright

(Article begins on next page)

12 October 2024

Available online at www.sciencedirect.com

ScienceDirect

Energy Procedia 126 (201709) 1107–1114

Energy Procedia

www.elsevier.com/locate/procedia

72nd Conference of the Italian Thermal Machines Engineering Association, ATI2017, 6-8 September 2017, Lecce, Italy

Comparison of Analytical and Numerical Methods for the Evaluation of the Flow Forces in Conical Poppet Valves with Direct and Reverse Flow

Massimo Rundo[a,*], Giorgio Altare[a]

[a]*Politecnico di Torino, Dipartimento Energia, C.so Duca degli Abruzzi 24, 10129, Torino*

Abstract

Different methods for the evaluation of the flow forces in conical poppet valves are analyzed. The equation derived from the conservation of the fluid momentum is contrasted with a formulation obtained from the Bernoulli's equation and with computational fluid dynamics (CFD) simulations performed through two commercial codes, PumpLinx and Flow Simulation. Three different poppet angles and two flow directions are analyzed. In some operating conditions, a significant difference was found between the analytical formulation and the outcomes of the CFD simulations in case of reverse flow.

© 2017 The Authors. Published by Elsevier Ltd.
Peer-review under responsibility of the scientific committee of the 72nd Conference of the Italian Thermal Machines Engineering Association

Keywords: Flow force; conical poppet valve; CFD

1. Introduction

Conical poppets are widely used as moveable elements for different types of fluid power valves, above all for pressure control. It is known that the steady-state performances of such valves are strongly affected by the flow forces, which modify the poppet equilibrium. For instance, in pressure relief and reducing valves, the effect of the flow force is the deviation of the regulated pressure from the theoretical value.

* Corresponding author. Tel.: +39-011-090-4406; fax: +39-011-090-4599.
E-mail address: massimo.rundo@polito.it

1876-6102 © 2017 The Authors. Published by Elsevier Ltd.
Peer-review under responsibility of the scientific committee of the 72nd Conference of the Italian Thermal Machines Engineering Association
10.1016/j.egypro.2017.08.261

Nomenclature

A_i, A_x	flow area at diameters d_i and d_x respectively	p_{in}, p_{out}	inlet / outlet pressure respectively
A_{min}	minimum flow area	Q	volumetric flow rate through the poppet valve
A_0	flow area at the inlet port	R	resultant force on a generic control volume
C_d	discharge coefficient	R_1, R_2	resultant forces on the control volumes 1 and 2
d_a	diameter for which the flow area is minimum	s	coordinate measured along a cone generatrix
d_i	diameter where the pressure starts to decrease	s_i	coordinate s in correspondence of the diameter d_i
d_r, d_s	rod / seat diameter respectively	s_{max}	coordinate s for which the flow area is minimum
d_x	diameter at a generic coordinate s	v_i, v_x	fluid velocity at diameters d_i and d_x respectively
D	diameter of the balancing cylinder	v_k	component of the fluid velocity in the k-th port
F_{CFD}	force on the cone simulated through CFD codes	v_{jet}	maximum fluid velocity in the vena contracta
F_c	force on the cone calculated analytically	v_{out}	fluid velocity at the outlet port
F_f	flow force	x_k	position of the k-th port of a control volume
F_p	theoretical static pressure force on the poppet	α	half-angle of the conical poppet
h	poppet lift	ρ	fluid density

Many studies have been carried out on flow forces in spool type elements, used for direction control and proportional valves. In these cases, the steady-state term of the flow force tends to close the valve regardless of the flow direction. Different techniques have been developed over the years to mitigate this undesired behaviour. On the contrary, the research on conical poppet valves is more limited, moreover different studies have demonstrated that under some circumstances the steady-state term acts in order to open the valve, above all when the flow is from the base to the apex of the cone (convergent flow). Since usually in such valves the normal flow direction is from the apex to the base (divergent flow), most studies have analysed only this operating condition.

It is common practice to use the equation derived from the conservation of the fluid momentum, originally developed for the spool valves, and assuming as jet angle the half-angle of the cone. However some studies have highlighted as such a formulation can lead to completely wrong results. Johnston et Al. [1] made experimental tests on conical poppet valves with divergent flow and they found conditions where the flow force tends to open the valve, due to the formation of a low pressure gradient on the rear face of the poppet. Other studies [2] have shown that the flow force is significanlty influenced by the cavitation in the downstream volume. The cavitation behind the poppet was investigated by other authors such as Hong et Al. [3]. It is evident that if the rear of the cone is exposed to a pressure field with levels lower than at the outlet port, an additional force, not taken into account by the conservation of the momentum, origines. It is known that the flow force is caused by a local pressure reduction as the fluid approaches the metering edge. Hence an alternative method for its evaluation is the determination of the pressure distribution along the cone between the inlet port and the minimum flow area. The most suitable method is through a 2D or 3D CFD analysis, however also analytic approaches can be used. For instance, Yang et Al. [4] implemented a simplified model for describing the pressure distribution on the poppet surface, using arcs of ellipse as isobaric surfaces. For the reverse flow, usually indicated as “convergent”, it is common practice to use the same analytic equation for the direct flow, assuming that the flow force acts always to close the valve [5, 6]. However, based on the theory of the fluid momentum, the force tends to open the valve [7]. Moreover, if a control volume downstream from the metering edge is considered, the expression of the flow force does not depend of the cone angle [8], since the oil leaves the control volume with axial direction. Experimental studies were carried out by Oshima [9] on different types of conical poppet valves. In case of sharp edge seat, the flow force tends to open the valve and, when the cavitation occurs, the magnitude of the force is increased, even if its absolute value remains lower than the theoretical force coming from the conservation of the fluid momentum. An additional term of the opening force is due to the overpressure in the proximity of the cone vertex, as also measured experimentally by Oshima et Al. [10]. In this paper two different analytic methodologies for the evaluation of the flow forces are contrasted. Moreover the high-end CFD sofware PumpLinx®, specific for hydraulic pumps, is compared with the tool Flow Simulation of the popular 3D CAD modeller Solidworks® for assessing the capability of the two products, in terms of both results and computational times.

2. Theoretical analysis

2.1. Fluid momentum approach

The 2nd Newton's law states that the resultant of the external forces acting on a system equates the time derivative of its momentum. In a valve, only the force component along the poppet axis has an influence on the equilibrium. For a given control volume with N ports located at a distance x_k along the valve axis from the origin of the reference system, the resultant of the forces acting on the volume itself is:

$$R = \rho \cdot \sum_{k=1}^{N} \left(v_k \cdot Q_k + x_k \cdot \frac{dQ_k}{dt} \right) \tag{1}$$

where the flow rate is positive if outgoing. Figure 1a shows a conical poppet valve with divergent (direct) flow, while in Figure 1b an example of valve with convergent flow is reported. With divergent flow, if the Eq. (1) is applied in steady-state conditions to the control volume with unit width, whose detail is shown on the right, only the interfaces 1-2 and 3-4 must be considered:

$$R = -F_f = R_{12} + R_{34} = \rho \left(v_{jet} \cos\alpha \cdot Q + 0 \cdot Q \right) = \rho Q v_{jet} \cos\alpha \tag{2}$$

Therefore the force F_f exerted by the fluid on the poppet has an opposite sign and tends to close the valve.

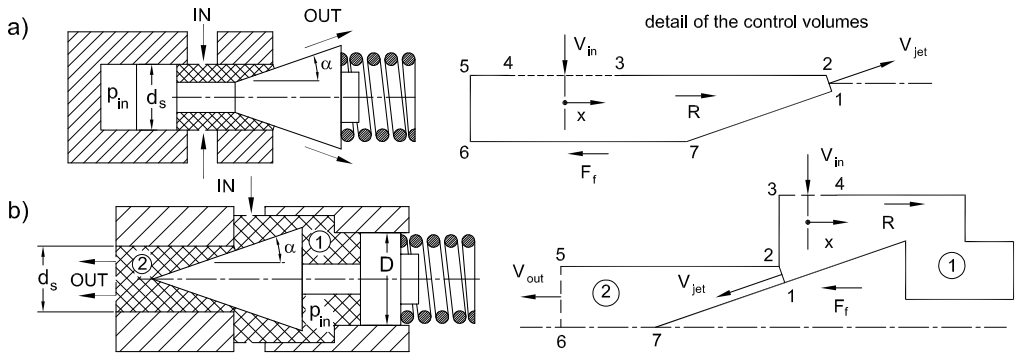

Figure 1: (a) conical poppet valves with divergent flow and (b) convergent flow with the detail of the control volumes on the right.

With convergent flow, if only the upstream control volume 1 is considered, the external force R_1 (see Eq. (3)) acting on the fluid has the same magnitude of the force expressed by the Eq. (2) but with opposite sign. However, the jet is deviated further before leaving the valve and such a deviation involves the surface of the poppet, hence an additional force arises downstream from the metering edge. To take into account this force, a second control volume 2 must be considered and the corresponding force acting on it is R_2 given by the Eq. (4). Therefore, the total force in case of convergent flow is given by the Eq. (5).

$$R_1 = R_{12} + R_{34} = \rho \left[0 \cdot (-Q) + \left(-v_{jet} \cos\alpha \right) \cdot Q \right] = -\rho Q v_{jet} \cos\alpha \tag{3}$$

$$R_2 = R_{12} + R_{56} = \rho \left[\left(-v_{jet} \cos\alpha \right) \cdot (-Q) + \left(-v_{out} \right) \cdot Q \right] = \rho Q \left(v_{jet} \cos\alpha - v_{out} \right) \tag{4}$$

$$R = -F = R_1 + R_2 = -\rho Q v_{out} = -4\rho Q^2 / \left(\pi d_s^2 \right) \tag{5}$$

It is evident that the force tends to open the valve and its magnitude is significantly lower with respect to the case with divergent flow, being the velocity v_{out} certainly smaller than v_{jet}.

2.2. Bernoulli's law approach

The flow force is due to the non-homogeneous pressure distribution on the cone surface. In case of divergent flow, it is quite easy to evaluate analytically the pressure distribution starting from the Bernoulli's law. With

reference to Figure 2, the pressure and the velocity of the fluid in correspondence of the cross section A_0 are p_{in} and v_{in} respectively. As the diameter of the cone increases, the fluid velocity grows with the reduction of the flow area A_x. It is possible to study the flow through a convergent annular pipe starting from the maximum area A_i with an inclination equal to α/2 up to the minimum area identified by the metering edge. A coordinate system s identifies the generic diameter d_x along the cone surface. The origin is in correspondence of the connection of the cone with the rod or in correspondence of the cone apex if the rod is not present. It can be assumed that in the cross section A_i the velocity and the pressure values are equal to the corresponding values in the section A_0.

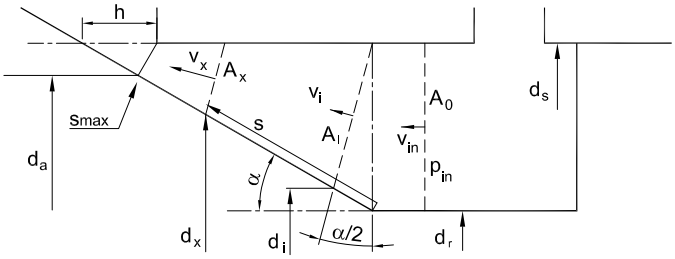

Figure 2: reference system for the analytic evaluation of the pressure distribution on the conical surface

The flow area in correspondence of the generic coordinate s and of the diameter d_x is:

$$A_x = \frac{d_s^2 - \left(d_r + 2s\sin\alpha\right)^2}{4\cos\left(\alpha/2\right)}\pi \tag{6}$$

If the Bernoulli's law is applied between the inlet section and the generic coordinate s, the local pressure is:

$$p_x = p_{in} + \rho Q^2\left(1/A_0^2 - 1/A_x^2\right)/2 \tag{7}$$

The axial force (8) on the conical surface is calculated by integration of the pressure p_x over the infinitesimal area with diameter d_x, where s_i is in correspondence of the diameter d_i and s_{max} at d_a where the flow area is minimum.

$$F_c = \pi\sin\alpha\int_{s_i}^{s_{\max}} p_x\left(d_r + 2s\sin\alpha\right)ds + p_0\frac{d_i^2 - d_r^2}{4}\pi \tag{8}$$

$$s_i = \frac{d_s - d_r}{2}\tan\left(\alpha/2\right) \quad ; \quad d_i = 2s_i\sin\alpha + d_r \tag{9}$$

$$s_{\max} = \frac{d_a - d_r}{2}\sin\alpha \quad ; \quad d_a = d_s - 2h\sin\alpha\cos\alpha \tag{10}$$

Finally, the flow force is the difference between the pressure on the base of the cylinder and on the conical surface:

$$F_f = p_{in}\left(d_s^2 - d_r^2\right)\pi/4 - F_c \tag{11}$$

2.3. Comparison between analytical models

The analytic models based on the change of the fluid momentum and on the Bernoulli's law have been contrasted for the case of divergent flow. The flow force given by the Eq. (2) can also be expressed by the Eq. (12), where A_{min} is the minimum flow area. The geometric parameters used for the comparison are d_s = 8 mm and d_r = 0 mm.

$$F_f = 2C_d A_{\min} p_{in}\cos\alpha \quad ; \quad A_{\min} = \pi h\sin\alpha\left(d_s - h\sin\alpha\cos\alpha\right) \tag{12}$$

The same inlet pressure p_{in} has been used for the two models evaluated as follows:

$$p_{in} = \frac{\rho}{2}\left(\frac{Q}{C_d A_{\min}}\right)^2 \tag{13}$$

In Figure 3a the comparison is shown as function of the poppet lift h, while the inlet pressure is plotted in Figure 3b. A good agreement has been found with the exception of the case with α = 45° and small openings. An error greater than 10% is also observed in case of high flow rates and high poppet lifts with low cone angles. Probably in such conditions the assumption that the pressure p_x is constant over the section A_x for any value of s is no longer valid.

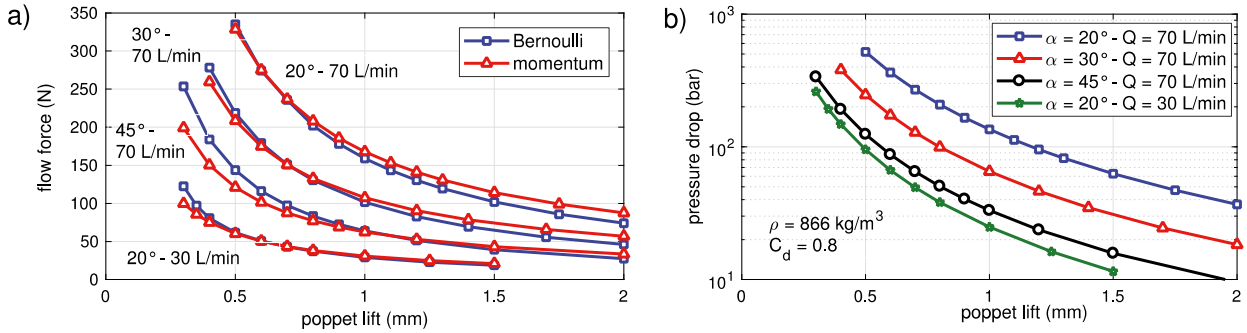

Figure 3: (a) flow force and (b) pressure vs. poppet lift with two different models, three poppet angles and two flow rates

3. CFD modeling

For the evaluation of the flow forces through CFD techniques, the poppets shown in Figure 4a were built in Solidworks 2016. For the divergent flow, an axial inlet was used, while the outlet port was located on the lateral surface of a cylinder. A geometry with a radial inlet, as shown in Figure 1a, was also tested, but with a negligible variation in terms of poppet force. The flow force was calculated as difference between the nominal static pressure force and the simulated force F_{CFD} on the conical surface (positive if it tends to close the valve):

$$F_f = \left(d_s^2 \pi / 4\right) p_{in} - F_{CFD} \tag{14}$$

For the convergent flow, a valve similar to the scheme in Figure 1b was created with $D = d$, so that also in this case the Eq. (14) gives the flow force, as long as the inlet pressure p_{in} is substituted by the outlet pressure p_{out}.
PumpLinx is the most advanced software for the simulation of pumps, although also semi-empirical models can be efficiently used for system-level simulations [11]. For the grid generation, the surfaces of the computational domain in STL format generated in Solidworks were imported. In the present study, the standard k-ε turbulence model and the 1st order upwind interpolation scheme were set. Different cavitation/aeration models are available, but the *Equilibrium Dissolved Gas* is the most used [12]; it evaluates the density of the oil/gas mixture based on the current volume fractions of dissolved/separated gas and on the local pressure value using the Henry's law. The aeration and dissolution phenomena are assumed instantaneous. The reliability of the cavitation model was proved experimentally in other studies [13] on gerotor pumps [14]. Six different models for direct and reverse flow and half-poppet angles α = 20°, 30° and 45° degrees were created. In order to maintain the same flow area, the poppet lift was set at 1 mm, 0.684 mm and 0.484 mm respectively. The flow rate was imposed as boundary condition at the valve inlet, while a pressure value was set at the outlet. In Figure 4b, the model in PumpLinx with the detail of the mesh in the metering edge is shown. A double local grid refinement was generated along the cone surface and in correspondence of the minimum flow area. The models are constituted by about 1.5 million cells. The simulations were performed with 5% of air volume fraction and the saturation pressure was set in order to have a Bunsen coefficient of 0.09. On a workstation with an eight-core Xeon processor at 3.4 GHz, the time required for a single simulation ranges between 20 min and 1 hour depending on how fast the convergence is. The validation of the CFD approach in PumpLinx was carried out on a conical poppet pressure relief valve with deflector for flow force compensation and coupling between the pressure field and the equation of motion of the poppet. The details of the study are reported in previous publications [15, 16]. The authors are confident about the reliability of the tool, since one of the poppet models studied in the current paper for the divergent flow is a subcomponent of the pressure relief valve already validated. Hence, it is reasonable that the simulated flow force could be very close to the real value.

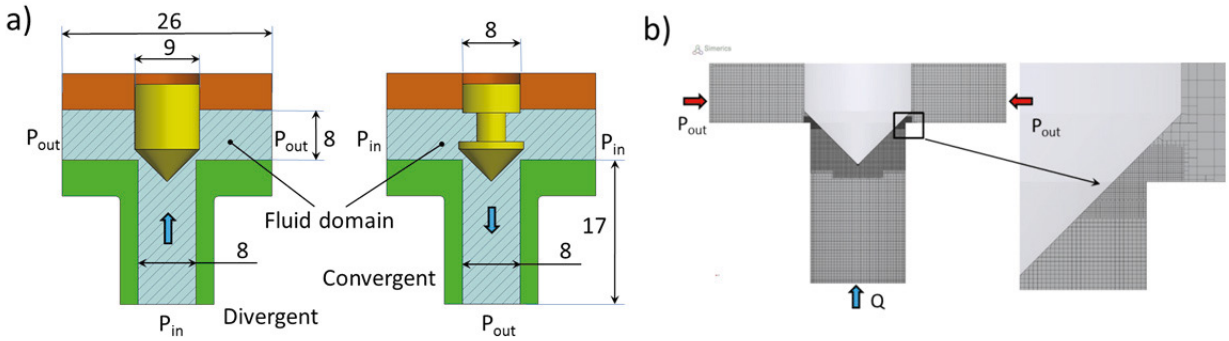

Figure 4: (a) geometry of the poppets for divergent and convergent flow and (b) model in PumpLinx for divergent flow and half-angle 45°

Flow Simulation® is the CAD-Embedded tool of Solidworks. For the turbulence, the Fabre-averaged Navier-Stokes equations are implemented with a low Reynolds k-ε Lam-Bremhorst model for closing the system of equations [17]. The spatial interpolation is of 2nd order, upwind limiters for the convective terms and central for diffusive terms. The same geometric configurations were created and the case with reverse flow and 45° is shown in Figure 5a. For the model developed in PumpLinx, the mesh independence analysis is reported in the reference [15], hence in this paper only the grid sensitivity of the Flow Simulation model is shown. In Figure 5b the flow force and the discharge coefficient are plotted as function of the number of cells. The base grid in region C is built with size 0.3 mm (level 1). Each refinement level (2-5) in regions B and A consists in dividing by 2 the side of the original cells. Satisfactory results are obtained with about 1.5 million cells as in PumpLinx. At equal number of cells, the CPU time is higher with respect to PumpLinx. The convergence is obtained in about 3-4 hours using 5 cores.

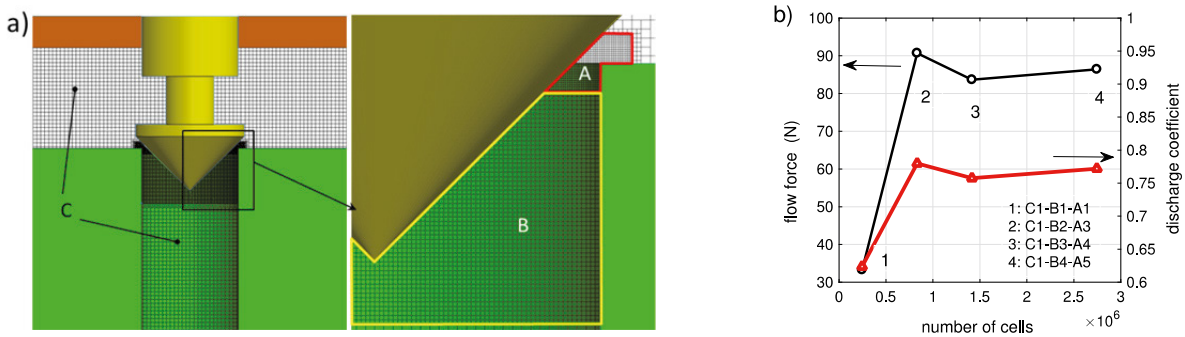

Figure 5: (a) model in Flow Simulation for convergent flow and half-angle 45° and (b) influence of the number of cells on the flow force and on the discharge coefficient with convergent flow, 70 l/min and angle of 45°

4. Results

Two different flow rates (30 and 70 l/min) were imposed at the inlet port, while at the outlet the atmospheric pressure was set. With convergent flow, the simulations in PumpLinx were performed also with a back pressure of 50 bar absolute in order to avoid the massive cavitation in the downstream chamber. It was checked that the back pressure has no influence in the evaluation of the force with divergent flow for the analyzed geometry, since the low pressure regions are located far away from the surface of the cone with no influence on the axial component of the poppet force. The synthesis of the results is presented in Figure 6. The flow force was calculated by means of the Eq. (14) for the CFD simulations. For the Eq. (12), used also in substitution of the Eq. (3) with the sign reversed, the pressure drop and the discharge coefficient were evaluated by the corresponding simulations in PumpLinx. With divergent flow and back pressure of 50 bar, the Eq. (12) that takes into account only the upstream control volume gives completely wrong results, on the contrary with the Eq. (5) the results are aligned with the CFD simulations.

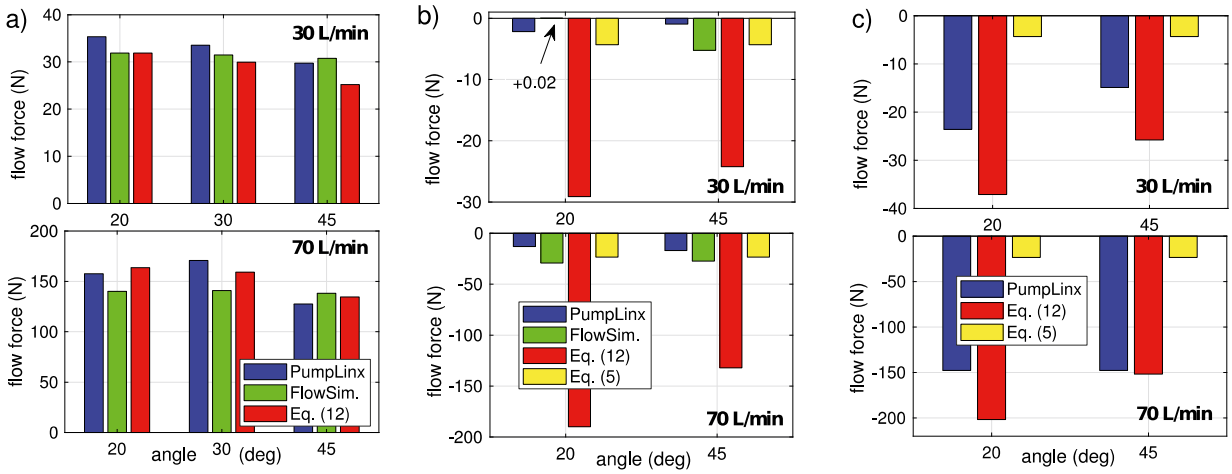

Figure 6: (a) flow force with divergent flow, (b) with convergent flow and back pressure and (c) with convergent flow without back pressure

By the analysis of the pressure field around the metering edge (Figure 7a), it is possible to understand the nature of the resultant force R_1. Most of the pressure gradient is located downstream from the diameter d_s, which represents the sealing diameter when the valve is closed. Hence, with respect to the condition of valve shut, a pressure distribution exists on an additional annular surface *a*, generating an opening force. However after this region of high gradient, the pressure does not simply tend to the outlet value, but continues to decrease in the region *b*. The reason is the increment of the flow area as the cone diameter decreases and the poppet behaves as a hydraulic diffuser. The fact that the pressure acting on a significant surface of the cone can fall below the outlet value (up to 15 bar lower) generates a force that tends to close the valve. An additional contribution is due to the pressure increment on the cone vertex (region *c*), which generates an opening force. In fact, the flow paths along the cone generatrixes gather in correspondence of the apex and the fluid is further deviated. This effect is higher with the half-angle 45° since the flow paths meet with an angle of 90°. However, since the surface involved by this last deviation is quite small due to the low diameter, the resultant of the force acting on the cone surface belonging the control volume 2 tends to close the valve and this contribution compensates most of the opening force relative to the control volume 1. On the contrary, without the back pressure, the expansion downstream from the metering edge leads to cavitation and the minimum pressure in the 2nd control volume is limited to 0 absolute bar (Figure 7b). The consequence is a limitation of the closing force that can compensate only partially the opening force on the annular surface *a*. Moreover, the overpressure on the region *c* is incremented by the higher fluid velocity along the cone due to the reduction of the discharge coefficient in cavitating conditions. Therefore at 70 l/min and with an angle α=45° the maximum opening force is reached and in this case best results are obtained with the term R_1 in the Eq. (3). However, in other operating conditions such as with 30 l/min, the results of the CFD simulation are intermediate between the Eqs. (3) and (5).

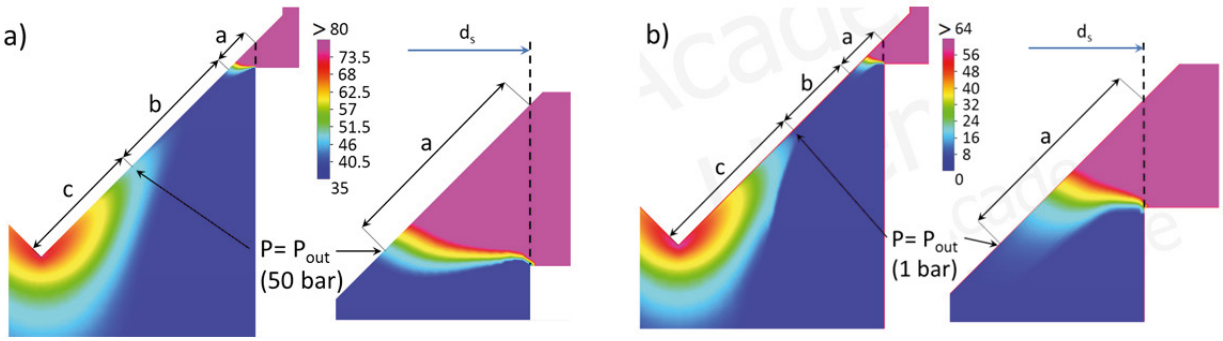

Figure 7: (a) pressure field on the conical poppet for convergent flow with back pressure of 50 bar and (b) without back pressure

5. Conclusions

Different methods for the evaluation of the flow forces in conical poppet valves with sharp edge seat have been discussed. Analytical methods have been contrasted with CFD analyses performed with two different commercial codes. It is shown that the divergent flow represents a quite easy case study; in fact, the simplified analytic evaluation of the pressure profile along the cone gives acceptable results in comparison to the method derived from the conservation of the momentum and also with respect to the CFD simulations. Moreover, no cavitation model is needed for the correct evaluation of the flow force, since even without a back pressure, the cavitation occurs in a region far away from the cone surface. In case of convergent flow, the region downstream from the metering edge must be also considered. Moreover, the flow force on the poppet is highly influenced by the cavitation, which modifies the pressure distribution along the cone downstream from the metering edge. In this case, a significant difference has been found between the analytical formulation and the outcomes of the CFD simulations. Although one of the CFD codes has already been validated on the steady-state characteristic of a pressure relief valve, it would be interesting to quantify by means of focused experimental tests the accuracy of the software in the evaluation of the flow force in case of convergent flow.

References

[1] Johnston DN, Edge KA, Vaughan ND. "Experimental investigation of flow and force characteristics of hydraulic poppet and disc valves". *Proc. IMechE Part A: Journal of Power and Energy* 205 (1991): 161-171. DOI: 10.1243/PIME_PROC_1991_205_025_02.

[2] Johnston DN. "Numerical modelling of reciprocating pumps with self-acting valves". *Proc. IMechE Part I: Journal of Systems and Control Engineering* 205(2) (1991): 87-96. DOI: 10.1243/PIME_PROC_1991_205_318_02.

[3] Hong G, Xin F, Hua-yong Y. "Numerical investigation of cavitating flow behind the cone of a poppet valve in water hydraulic system". *Journal of Zhejiang University - SCIENCE A* 3(4) (2002): 395-400.

[4] Yang Y, Wu J, Feng F, Zhu Y. "Flow characteristics of throttle valve with sharp-edged seat". *Proceedings of the International Conference on Fluid Power and Mechatronix*, Beijing, China.

[5] Muller MT, Fales RC. "Design and Analysis of a Two-Stage Poppet Valve for Flow Control". *Int. Journal of Fluid Power* 9(1) (2008): 17-26. DOI: 10.1080/14399776.2008.10781293.

[6] Opdenbosch P, Sadegh N, Book W, Murray T, Yang R. "Modelling an Electro-Hydraulic Poppet Valve". *Int. Journal of Fluid Power* 10(1) (2014): 7-15. DOI: 10.1080/14399776.2009.10780963.

[7] Weixiang S, Binggang C, Zhiyong T. "Review and progress on flow force of a poppet valve". *Proceedings of the JFPS International Symposium on Fluid Power*, Tokyo, Japan.

[8] Kasai K. "On the stability of a poppet valve with an elastic support". *Bulletin of JSME* 11(48) (1968): 1068-1083.

[9] Oshima S. An experimental study on the several poppet valves with difference in shape". *Proceedings of the JFPS International Symposium on Fluid Power*, Tokyo, Japan.

[10] Oshima S, Leino T, Linjama M, Koskinen KT, Vilenius MJ. "Effect of Cavitation in Water Hydraulic Poppet Valves". *Int. Journal of Fluid Power* 2(3) (2001): 5-13. DOI: 10.1080/14399776.2001.10781115.

[11] Casoli P, Anthony A, Rigosi M. "Modeling of an Excavator System - Semi empirical hydraulic pump model". *SAE Int. J. Commer. Veh.* 4(1) (2011): 242-255. DOI: 10.4271/2011-01-2278.

[12] Singhal A, Athavale M, Li H, Jiang Y. "Mathematical Basis and Validation of the Full Cavitation Model". *ASME J. Fluids Eng.* 124(3) (2002): 617–624. DOI:10.1115/1.1486223.

[13] Altare G, Rundo M. "Computational Fluid Dynamics Analysis of Gerotor Lubricating Pumps at High-Speed: Geometric Features Influencing the Filling Capability". *ASME J. Fluids Eng* 138(11) (2016): 111101. DOI: 10.1115/1.4033675.

[14] Rundo M, Nervegna N. "Lubrication Pumps for Internal Combustion Engines: a Review". *Int. Journal of Fluid Power* 16(2) (2015): 59-74. DOI: 10.1080/14399776.2015.1050935.

[15] Altare G, Rundo M, Olivetti M. "3D Dynamic Simulation of a Flow Force Compensated Pressure Relief Valve". *Proceedings of the ASME International Mechanical Engineering Congress and Exposition,* Phoenix, USA. DOI: 10.1115/IMECE2016-65624.

[16] Finesso R, Rundo R. "Numerical and experimental investigation on a conical poppet relief valve with flow force compensation". *Int. Journal of Fluid Power* 18(2) (2017). DOI: 10.1080/14399776.2017.1296740.

[17] Sobachkin A, Dumnov G. "Numerical Basis of CAD-Embedded CFD". *Proceedings of the NAFEMS World Congress,* Salzburg, Austria.